

Submitted: 03/02/2025

Revised: 13/04/2025

Accepted: 19/04/2025

Published: 31/05/2025

Histomorphometry of limb skeletogenesis in prehatched precocial embryos (Japanese quail and Cochin chicken) and altricial embryos (racing pigeons and cockatiel birds)

Iftikhar Mohammed Abdul Karim  and Ramzi Abdulghafoor Al-Agele* 

Department of Anatomy and Histology, College of Veterinary Medicine, University of Diyala, Baqubah, Iraq

Abstract

Background: Birds are the group of tetrapods that exhibit the greatest diversity in taxonomy and ecology. Limb development is a major focus of developmental and evolutionary biology research.

Aim: This study characterized the variances in histomorphometry of skeletogenesis in precocial embryos, such as Japanese quail (Jq) and Cochin chickens (Cc), and altricial embryos, including Racing pigeons (Rp) and Cockatiel birds (Cb).

Methods: Six embryos were collected on days 8, 10, 12, 14, 16, and 18 of incubation. Three embryos were prepared and stained with Alcian Blue for chondrification and Alizarin Red for ossified bones. The remaining three embryos were subjected to histological evaluation.

Results: Initial signs of ossification appeared in the femur, tibiofibular, and humerus bones of Jq, Rp, and Cb embryos on day 8 and in the bones of Cc on day 10. The statistical study revealed that embryos of different developmental days had considerable variations in average ossified lengths for the humerus of the forelimb, especially Rp, and the femur of the hindlimb, notably in Jq. On day 8, microscopic examination revealed a hypertrophic area with enlarged chondrocytes in the middle and sides of the diaphysis. Osteoblasts significantly augmented the periosteal bone collar around the mid-diaphysis, enhancing its thickness toward the diaphysis center; by day 16, the primary woven bone had developed.

Conclusion: This study highlighted the growth rate of the hind limb in precocial embryos, particularly in Jq, which was higher than that in other embryos. These data serve as essential indicators and indispensable parameters for interpreting and elucidating the data collected in these studies.

Keywords: Avian embryo, Chondrification, Limb development, Osteogenesis, Skeletogenesis.

Introduction

Birds modify the shapes of their limb bones to withstand the forces generated during movement (McGuire *et al.*, 2020). Both developmental and evolutionary biology now consider the process of limb formation in vertebrates, with a significant focus on evolutionary biology on the transition from the fin to the limb (Sears *et al.*, 2018; Watanabe, 2018). Birds are the group of tetrapods that exhibit the greatest diversity in taxonomy and ecology (Xu *et al.*, 2014). The forelimbs (FL) have evolved into wings primarily for flight, while the legs serve as a mechanism for bipedal movement (Gillian, 2000; Watanabe, 2018). Some studies indicate that altricial birds are distinguished by the swift early maturation of “supply” organs, including digestive systems. Conversely, precocial birds have accelerated the early development of many “demand” tissues, including the muscular, nervous, skeletal, and feathers (Dial and Carrier, 2012;

Augustine *et al.*, 2019). The morphological process of embryonic development is responsible for the majority of skeletal features in the avian limb. Nevertheless, certain morphological alterations, such as fusion and distortion of the skeletal structure, occur during the latter stages of development or after hatching (Seki *et al.*, 2012). Birds develop and increase the size of their bones through intramembranous and endochondral ossification (Nie *et al.*, 2019). Endochondral ossification is the process by which mesenchyme cells convert into cartilage templates and then into bones. On the other hand, intramembranous ossification involves the direct conversion of mesenchyme cells into bone tissue (Ahmed and Soliman, 2013). Osteogenesis, also known as ossification, is a biological process involving the formation of new bone. Chondrogenesis is the initial stage of skeletal development. It occurs during embryonic development in the early phases of somitogenesis and leads to the formation of the first

*Corresponding Author: Ramzi Al-Agele. Department of Anatomy and Histology, College of Veterinary Medicine, University of Diyala, Baqubah, Iraq. Email: al-agele@uodiyala.edu.iq

skeletal bones (Gao *et al.*, 2018). Bone growth forms the body scaffold through a series of synchronous actions. During maturation, the bone and the surrounding environment, which includes Schwann, endothelial, and inflammatory cells, remain active throughout adulthood, facilitating the return of tissue to its homeostatic functioning condition (Salhotra *et al.*, 2020). Appositional development occurs inside the periosteal plate, and interstitial cartilage growth in the epiphyseal plate is responsible for bone growth (Gao *et al.*, 2018; Li *et al.*, 2024). The developing embryo's somatic mesoderm is responsible for producing the skeletal components of the limbs. The somatic mesoderm originates from a single layer of the lateral plate mesoderm during the ontogenetic development process. As a result, the celom divides into two distinct layers (Prummel *et al.*, 2020). Although a substantial amount of information is available on these systems, the mechanism responsible for producing the distinct skeletal structure and arrangement of limbs in birds is still not well understood (Seki *et al.*, 2012). During adulthood, bone remodeling is a regulated and balanced process involving osteoclasts, which break down bone, and osteoblasts, which build new bone. This process helps maintain bone homeostasis (Regatta and Artridge, 2010). During embryogenesis, osteoblasts release a matrix, some of which embeds inside newly created bone. Then, they change into osteocytes, which help bones grow through ossification that occurs inside or outside the membrane (Chan *et al.*, 2021). Bone homeostasis is an intricate process in which osteoclasts break down bone and generate new bone tissue. Precise control and coordination of this process are crucial for preserving bone integrity (Al-Agele *et al.*, 2021). Osteoclasts are large, multinucleated cells originating from hematopoietic cells in the bone marrow. They play crucial roles in preserving the equilibrium of the skeletal system and producing blood cells (Ikeda and Takeshita, 2016). Multiple intricate functional and evolutionary aspects impact the formation and development of bone, which is a very intricate structure. For birds, this involves the difficulty of adapting their skeleton to both flying and walking on land, namely the requirements of supporting their weight while perching (Wu *et al.*, 2022). The gross anatomy of flightless avian species has been the subject of several studies and/or of other flightless avian species. Using an avian embryo as an experimental model in embryology offers benefits such as smaller size, faster prolificity, and precocity. Therefore, a list of natural embryonic developmental phases can serve as a normal control for conducting and assessing research using avian embryos and skeletal mutants. Thus, information about the normal stages of skeletogenesis in bird species is essential for understanding and interpreting data from embryology, developmental engineering, and teratology experiments (Kürtül *et al.*, 2009). Furthermore, numerous studies have routinely examined the pre-hatching development

of the avian skeletal system (Poullis *et al.*, 1998; Kürtül *et al.*, 2009; Wu *et al.*, 2022). However, histomorphometric investigations of bone development in flightless avian species have been limited, and their structural variances have been compared with those of other flight avian species. Therefore, this study aimed to determine the timing of chondrification and ossification in the FL and hindlimb (HL) bones and to compare these findings across different types of precocial embryos [Japanese quail (Jq) and Cochin chicken (Cc)] and altricial embryos [racing pigeons (Rp) and cockatiel birds (Cb)].

Materials and Methods

Experimental design

Fertilized eggs from each bird species, including Rp, Cb, Jq, and Cc embryos, were collected within 6 hours postlaying and kept at 15°C for approximately 5 days. The eggs were incubated in an incubator at a temperature of 37.7°C ± 0.2°C and 70% relative humidity. Six embryos were collected on days 8, 10, 12, 14, 16, and 18 of incubation. Three embryos from each day of incubation were prepared and subjected to double staining with Alcian Blue (AB) for chondrification and Alizarin Red (AR) for ossified bones. The remaining three embryos were subjected to histological evaluation. Embryos were collected for skeletal staining on days 8, 10, 12, 14, 16, and 18 of incubation, contingent upon the duration of incubation.

Principal steps of double-staining of the embryonic skeleton

The experimental embryos were double-staining with AB and AR for cartilage and ossified bones, respectively. This was done as stated by Nakane and Tsudzuki (1999). The initial stage of the evisceration process involved elimination of the thoracic and abdominal cavities. The samples were immersed in 90% ethanol for 7 days. Cartilage staining was performed using samples that were fully submerged and transferred into a solution of 0.01% AB, which was made using a mixture of 70 ml pure ethanol and 30 ml glacial acetic acid at a ratio of 7:3. Rehydration involved immersing the specimens twice in a 95% ethanol solution for 2 hours each. Each sample was then immersed in sequential baths with decreasing ethanol percentages: 75%, 40%, and 15% for 2 hours each. The embryos were washed in many rounds of distilled water for 2 hours. Clearing: the samples were immersed in a solution of 1% potassium hydroxide until the skeletal system of the embryo became visible. Bone staining: the specimen was immersed in a 0.001% aqueous solution of AR for 3 days. Next, the specimen was washed for 3 hours in a 1% potassium hydroxide solution. During the clearing and dehydration process, the items were subjected to increasing concentrations of glycerol in a solution containing 1% potassium hydroxide for 24 hours at each stage. The item was immersed in pure glycerin for

long-term preservation. To inhibit mold growth, thymol crystals were introduced into the storage solution.

Statistical analysis

All graphs were created using GraphPad software (Prism 6), and the results were presented as the mean ± SE using Excel software. The data collected by measuring the length of the ossified area as well as the data generated by measuring the entire length of the FL and HL using Fiji image software as described by (Al-Agele, 2020; Kadhim *et al.*, 2023; Nasser *et al.*, 2024) were analyzed by two-way ANOVA methods using GraphPad software (Prism 6). The statistical analysis of significant differences was used for comparisons in all studies, and the threshold for significance was set at $p < 0.05$.

Ethical approval

This study was carried out following the strictest standards regarding the main rules of care and the use of animals in research. The experiment was conducted according to the guidelines of the College of Veterinary Medicine, University of Diyala Animal Experimentation Ethics Committee (No. VM 154. October 2023. I&R) dated on 1/10/2023.

Results

Morphometric data

Sequential bone development was indicated by staining embryonic skeletons with AB, which imparted a blue hue to the chondrification zone, and AR, which rendered the ossification area red, as illustrated in Figure 4. AB staining indicated the transition from chondrification, denoted by blue, to ossification (red) in both the FL and HL skeletons. Table 1 presents the average measurement times (mean ± SE) for the development of the HL bones. The ossified length (O Le), region in red, and total length of the femur bone (F

Le). Additionally, the next calculation determines the ossified proportion (O Pr) by dividing the ossified area by the femur length at different stages of development, specifically E8, E10, E12, E14, E16, and E18.

Statistical analysis data

Statistically significant differences were observed in the skeletogenesis of the humerus and femur bones. Several statistically significant changes ($p < 0.05$) were identified regarding an increase in the length of the ossified region of the humerus with an increase in the incubation duration. All experimental birds showed significant changes with increasing length of the ossified region, which correlated with increasing duration of egg incubation (Fig. 1). Figure 2 illustrates the significant changes observed with increasing femur ossified region length. The lengths of the ossified humerus and femur bones of all four experimental birds was analyzed statistically. Figure 3 shows that the length of the humerus ossified region significantly changed with the time the eggs were incubated, with the results being observable in the Rp and Cc. On the other hand, the Jq ossified region of the femur differed significantly from that of the other three experimental birds.

Macroscopical results

This study found that on day 8 of incubation, staining the embryonic skeleton of Rp embryos with AB and AR highlighted the ossified area to turn red and the cartilaginous sections to turn blue (Fig. 4). These observations revealed that the ossified area had begun to form during the bone shift. Ossification of the ulna, radius, and humerus began (Fig. 4). The tiny center near the diaphysis shows an ossified portion with a reddish-brown tint. There is also a hint of a blue tint in the first phalanx of the alular digit. However, Cc did not show any signs of red staining, which were observed by day

Table 1. Morphometric data presented as (mean ± SE) in (mm) for the development of the hind limb bones. It shows the ossified length (O Le) and the overall length of the femur bone (F Le). It further computes the ossified proportion (O Pr) for various developmental stages (E8, E10, E12, E14, E16, E18), (N = 3 on each stage).

Embryo	Type	Traits	E8	E10	E12	E14	E16	E18
Precocial embryos	Jq	O Le	0.64 ± 0.38	1.28 ± 0.28	2.72 ± 0.16	4.10 ± 0.27	5.18 ± 0.08	6.12 ± 0.12
		F Le	5.12 ± 0.07	6.73 ± 0.09	6.99 ± 0.09	10.13 ± 0.17	12.48 ± 0.48	12.70 ± 0.42
		O Pr	0.13	0.19	0.39	0.40	0.42	0.48
	Cc	O Le	0.44 ± 0.25	1.01 ± 0.10	2.22 ± 0.16	4.4 ± 0.21	7.13 ± 0.57	7.96 ± 0.23
		F Le	2.09 ± 0.04	3.41 ± 0.21	5.85 ± 0.44	6.99 ± 0.54	7.85 ± 0.43	8.19 ± 0.34
		O Pr	0.29	0.36	0.47	0.51	0.65	0.72
Altricial embryos	Rp	O Le	0.62 ± 0.36	1.25 ± 0.26	2.76 ± 0.14	3.52 ± 0.25	5.12 ± 0.06	5.95 ± 0.10
		F Le	4.11 ± 0.06	5.03 ± 0.07	6.06 ± 0.12	6.57 ± 0.24	7.49 ± 0.25	8.33 ± 0.28
		O Pr	0.15	0.24	0.45	0.53	0.68	0.71
	Cb	O Le	0.48 ± 0.27	0.68 ± 0.21	1.26 ± 0.12	2.01 ± 0.04	2.46 ± 0.26	3.72 ± 0.10
		F Le	4.6 ± 0.05	4.93 ± 0.08	5.91 ± 0.10	6.39 ± 0.07	7.29 ± 0.10	7.97 ± 0.07
		O Pr	0.10	0.14	0.21	0.31	0.34	0.47

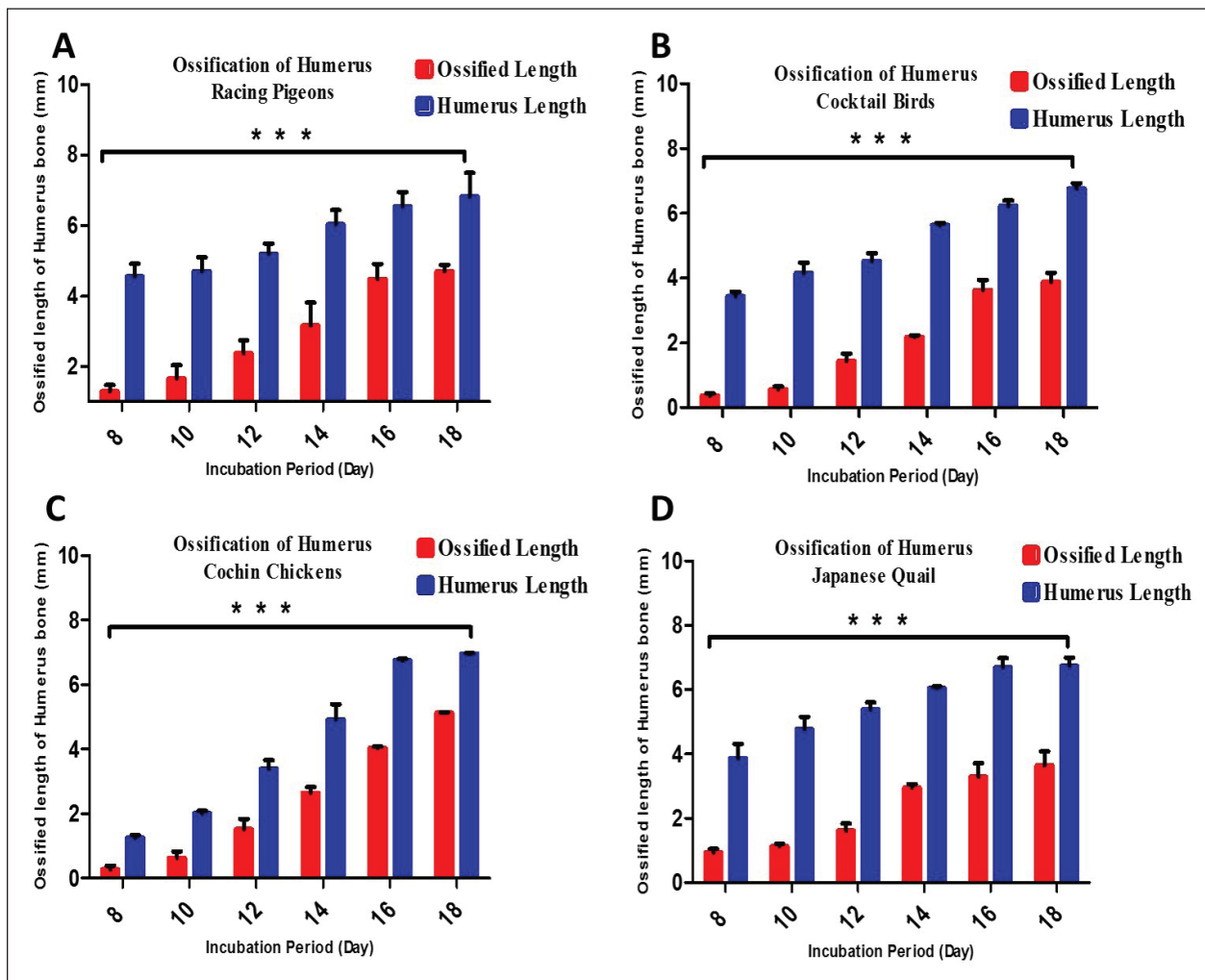


Fig. 1. Graphs showing the significant difference in the total length (blue color bars) and the length of the ossified part (red color bars) of the humerus for three embryos per day for 8, 10, 12, 14, 16, and 18 days of incubation of Rp (A), Cb (B), Cc (C), and Jq (D). The data are presented as (mean \pm SE) at $p < 0.05$.

10. This study found that on the teen day of incubation, staining the embryonic skeleton of Cb embryos with AB and AR caused the ossified area. Tarso-metatarsals II, III, and IV exhibit blue staining in the FL, whereas tarso-metatarsals II, III, and IV exhibit red staining in the HL. The carpi and metacarpi combine to form the composite carpometacarpal. After the pectoral girdle and wing components completed their development, the ossification component entered the extremities of the elements. The alular digit's second phalanx underwent blue staining. This study showed that staining the Rp embryo skeletons with AB and AR on day 12 of incubation caused an ossified area of the ulna, radius, humerus (FL), femur, and tibia (HL), which underwent ossification. Ossification of the ulna, radius, and humerus (FL), femur, and tibia (HL) occurred on the 14th day of incubation of Jq embryos. On day 16 of incubation, staining the embryonic skeletons of

Rp embryos revealed ossified regions where the 2nd phalanx of the alular digit underwent ossification. This study revealed that metacarpals III and IV of the FL exhibited a faint red stain at their middiaphyseal region, indicating the onset of ossification. On the 18th day of incubation, staining the embryonic skeletons of Rp embryos revealed an expansion of the ossified region, as shown in Figure 4. The ulna, radius, and humerus (FL), as well as the femur and tibia (HL), undergo ossification.

Microscopical results

The present study revealed that on day 8 of incubation, the cartilage template started to take on the shape of the potential humerus, complete with the middiaphysis and epiphyses at the end. The epiphyseal area was filled with tiny chondrocytes that were randomly dispersed throughout the extracellular matrix. These chondrocytes were observed in Rp, Jq, and Cb, which

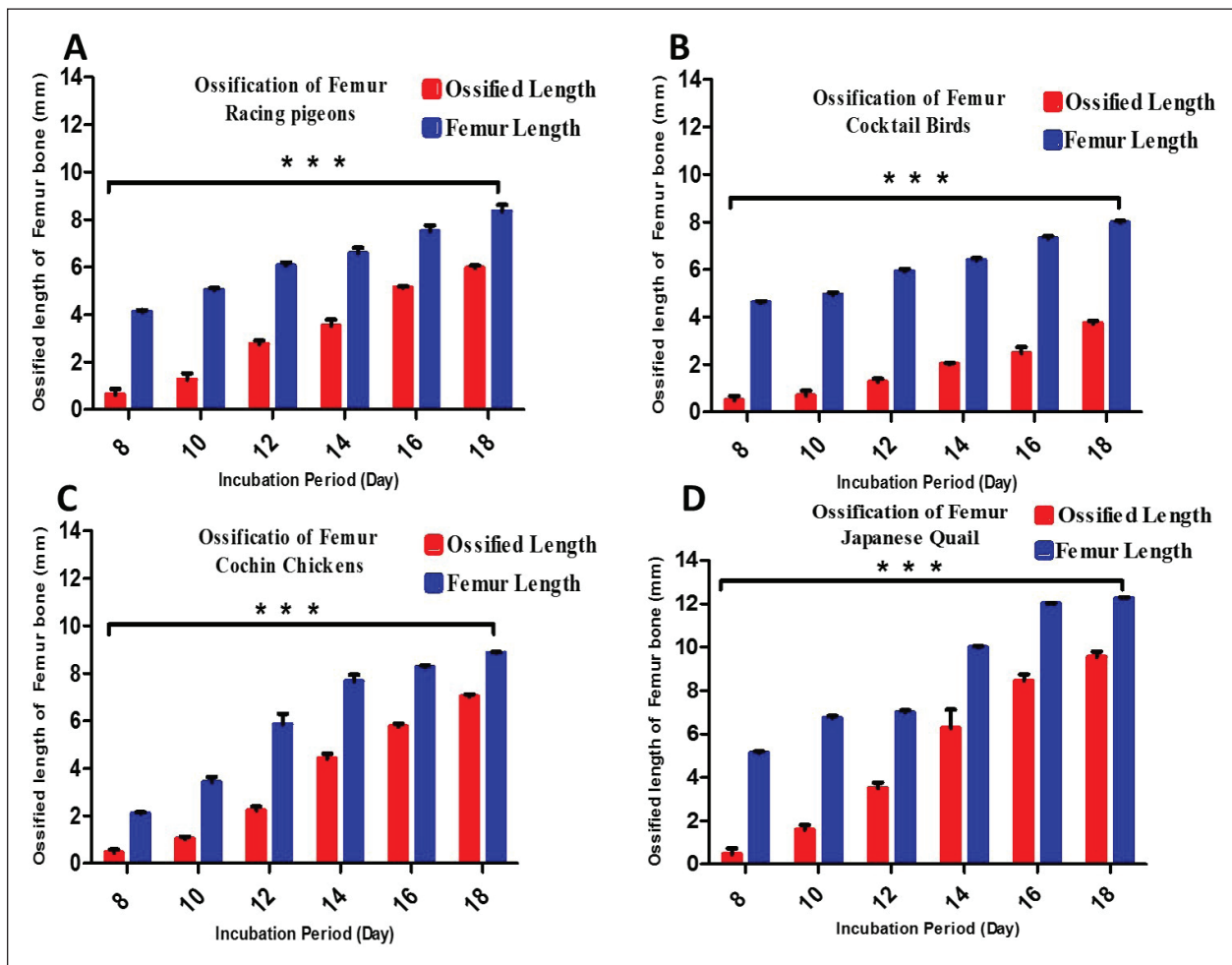


Fig. 2. Graphs showing the significant difference in the total length (blue color bars) and the length of the ossified part (red color bars) of the femur for three embryos per day for 8, 10, 12, 14, 16, and 18 days of incubation of Rp (A), Cb (B), Ccs (C), and Jq (D). The data are presented as (mean \pm SE) at $p < 0.05$.

were observed in very few areas in Cc embryos. These chondrocytes ranged in size from round to oval. The hypertrophic zone, which was composed of large chondrocytes, was observed in the middle of the diaphysis, as well as on both of the hypertrophic zone's boundaries. Additionally, the proliferative zone was composed of chondrocytes. The inner cellular layer of the perichondrium was differentiated into a few osteoblasts on the 8th day. In the middiaphysis region, where the chondrocytes had grown too large, these osteoblasts deposited osteoid tissue in the form of a bone collar on the 10th day. This caused the perichondrium to gradually transform into the periosteum (Fig. 5). The bone collar developed calcification on the 10th day. It was shown that in the mid-diaphysis region, where the chondrocytes had grown too large, the osteoblasts deposited osteoid tissue in the form of a bone collar, which caused the perichondrium to gradually transform into the periosteal. The results showed that

osteoblasts started to form osteoid tissue using the cartilage matrix as a base. Bone spicules began to form at the beginning of endochondral ossification. Consequently, these spicules interconnected, resulting in the formation of bone trabeculae on day 12. On the 14th day, the periosteal bone collar had more osteoblasts depositing around the middiaphysis and thickening toward the center of the diaphysis. Mature osteoblasts become stuck in the matrix and change into osteocytes, leading to the formation of primary woven bone on day 14. Calcification of the trabecular bone transpired on the sixteenth day. The endochondral bone trabeculae were more fully developed when they encountered the periosteal bone collar. They were located throughout the middiaphysis of the humerus. Changes in the development of long bones in the limbs were observable as early as the 18th day of incubation. These alterations caused the diaphysis to expand in both length and width. During resorption, the osteoclasts

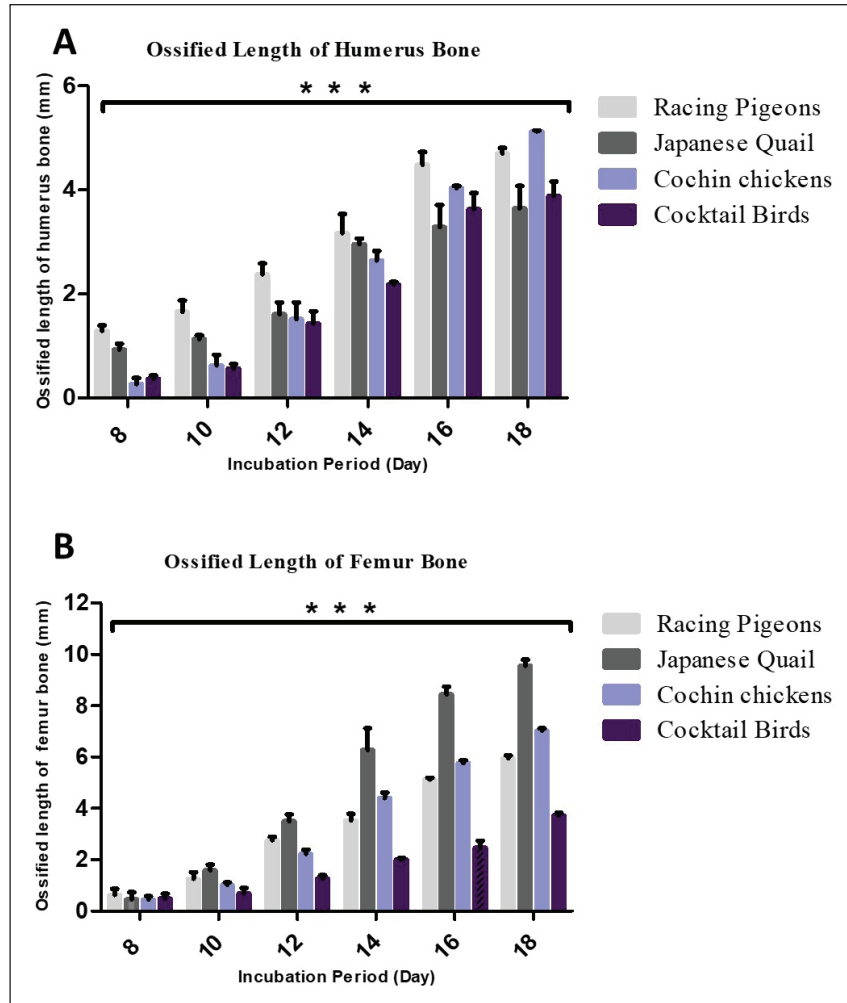


Fig. 3. Graphs showing the significant difference in the total length of the ossified part of the humerus (A) and femur (B) for three embryos per day for 8, 10, 12, 14, 16, and 18 days of incubation of Rps (light gray color bars), Jq (dark gray color bars), Ccs (blue color bars), and Cocktail birds (black color bars). The data are presented as (mean \pm SE) at $p < 0.05$.

dismantled the endochondral trabecular bone. This event initiated the formation of the bone marrow cavity in the middiaphysis on day 18.

Discussion

Anatomical study

HL calcification affects standing and movement during embryonic development (Poullis *et al.*, 1998). However, the FL holds the body during flight. Skeletons are the main body support. This study, which examined the skeletogenesis of different bird embryos, suggests that early embryonic skeletogenesis events may vary within and between species (Li *et al.*, 2024). The ground-dwelling Jq and Cc were compared in this study. Both birds require strong HL to walk, run, and fly. Nakamura *et al.* (2019) reported that the HL, like the Jq

and Cc bones, ossifies faster. However, quail embryos developed faster and matured when hatched. Wu *et al.* (2022) reported that pigeons develop faster than quails after hatching. This study demonstrated cartilage ossification in the quail femurs and tibiofibular bones on day 8 and in the Cc bones on day 10. Zorab and Salih (2021) reported that HL ossified continuously and progressively during embryonic development, with most of them ossifying before hatching, consistent with earlier studies (Nakane and Tsudzuki, 1999; Dial and Carrier, 2012). Rp and Cb spend much of their time flying. Thus, their FL must develop to generate flying power. As shown in Figure 1, the order and duration of chondrification and ossification for most FL and HL bones in Cb, Jq, Rp, and Cc are given. The calcification patterns of the FL, such as the humerus bone and HL

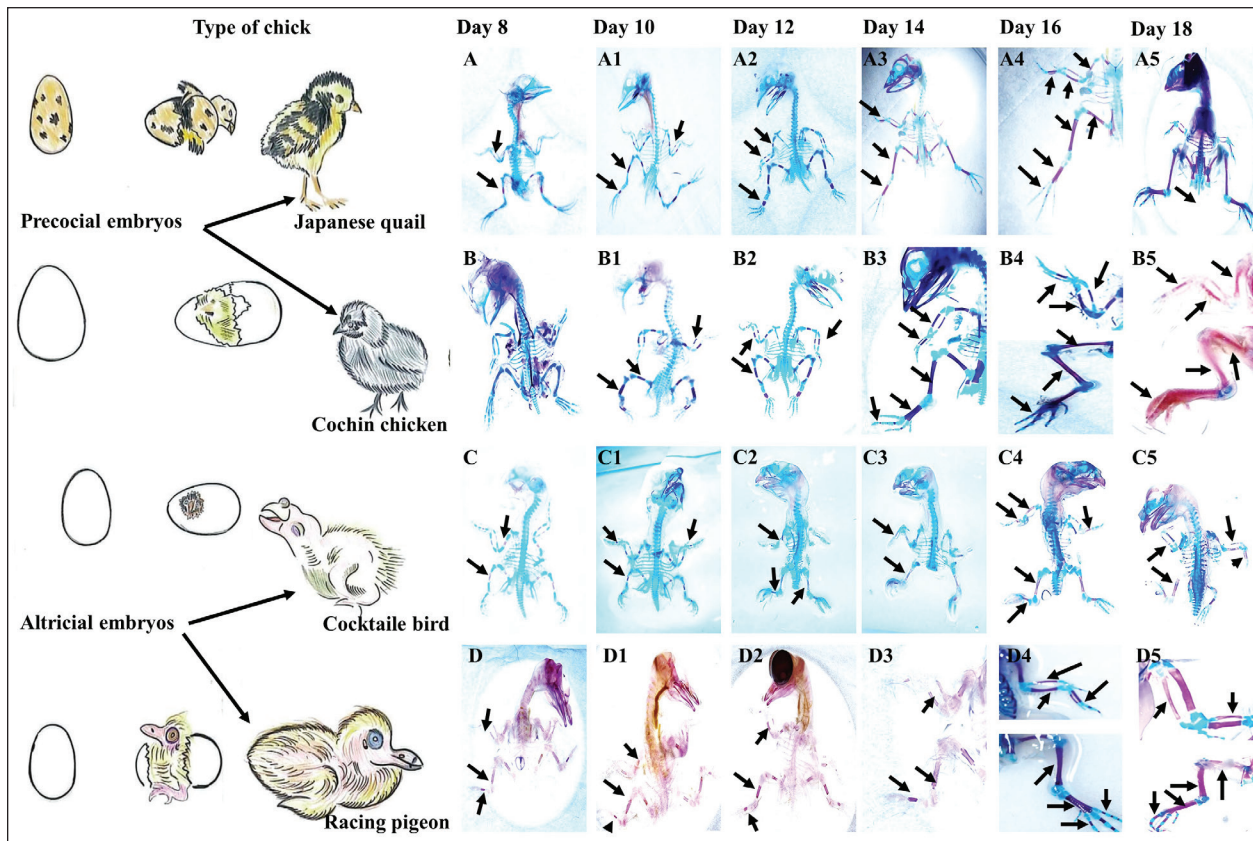


Fig. 4. Skeletogenesis of precocial, including Jq embryos (A-A5) and Cc embryos (B-B5) and altricial, including Cb embryos (C-C5) and Rp embryos (D-D5) illustrates the area of ossification in the embryo subjected to double staining with (AB) for chondrification and (AR) for ossified bones on days 8, 10, 12, 14, 16, and 18 of the incubation period. The ulna, radius, and humerus initiate ossification on day 8 in all embryos, except Cc embryos on day 10. The small, reddish-stained center near the diaphysis is the ossified portion (black arrows). Staining showed intense staining of the embryonic skeleton on the 18th day of incubation. The ulna, radius, and humerus ossify in the FL, whereas the femur and tibia form in the HL.

femur, showed variances in the skeletogenesis order of ossification. The embryonic bones of the Cb and Rp embryos showed calcification far later than those of humerus on Jq. However, Jq embryos form these bones, which are calcified later than normal bones. This calcification delay occurs between the terminal and first phalanges. Comparing a bird's FL and HL on the bone morphology and embryonic skeleton staining showed that Jq and Rp had different embryonic development patterns and hatching skeletal development rates. Different skeletal development rates explain these disparities in precocial and altricial embryos (Wu *et al.*, 2022). In contrast to other developmental features, the typical ossification sequence pattern is consistent. This is true even when FL and HL features evolve differently (Wu *et al.*, 2022). This is also true for precocial and altricial birds (Wei and Zhang, 2019). These findings suggest that animal locomotion is linked to limb-bone mechanical performance (Gillian, 2000). Jq hatchlings have completely formed HL, according to Nakane and Tsudzuki (1999). Pigeons prefer to fly but can dig and

feed on their back legs. This shows that the hatching Cc and Jq have different geometrical and mechanical femur bones than Rp and Cb. Wu *et al.* (2022) found stiff bone tissue in hatching quails. In reality, Jq, especially domesticated ones, are ground-dwellers, and their HL is essential for walking, running, and flying (Li *et al.*, 2024).

Histological study

The findings showed that by day 8, the hypertrophic zone was characterized by larger chondrocytes situated in the middle of the diaphysis and on each side of the hypertrophic zone. These results correspond with those of Zorab and Salih (2021), who reported that ossification in the humerus occurred on the 8th day. However, Nakane and Tsudzuki (1999) and Nishimura *et al.* (2012) reported that the first ossification center of these bones was observed on day 7. Additionally, Pourlis and Antonopoulos (2011) documented an extraordinary early ossification of these bones on the sixth day. However, these indicate potential species variance within the same genus, or that discrepancies

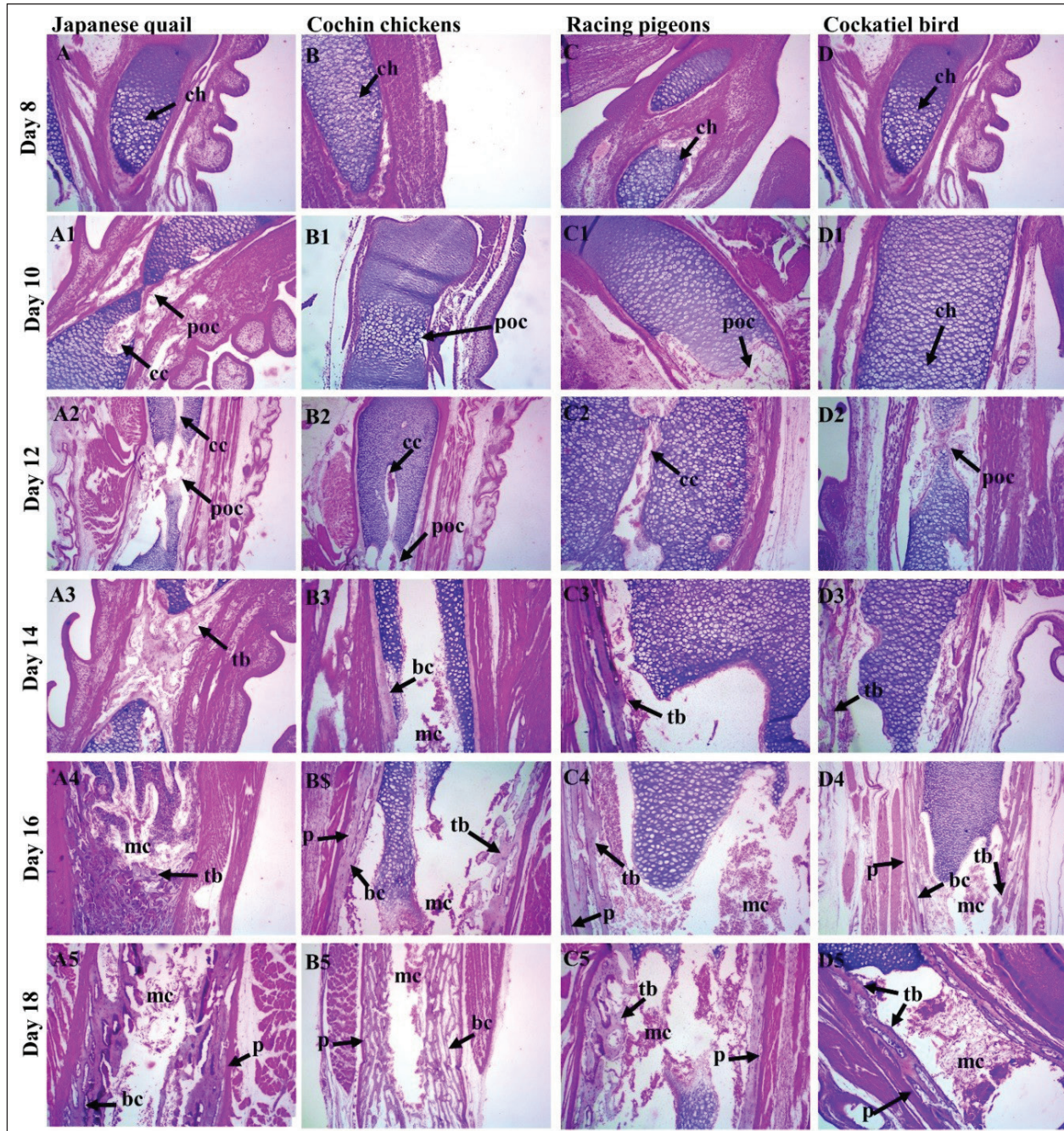


Fig. 5. A photomicrograph images of H & E stained tissue sections showing skeletogenesis of limb embryos, (A-A5) Jq embryos, (B-B5) Cc embryos, (C-C5) Rp embryos, (D-D5) Cb embryos, of 8, 10, 12, 14, 16, and 18-day-old embryos. The hypertrophy zone, characterized by larger chondrocytes (ch) and associated with the formation of the cartilage canal (cc), primary ossification center was located in the center of the diaphysis, Cartilage canal (cc); as the embryo progressed, the trabecular bone (tb) and bone collar (bc) forming in the center the medullary cavity (mc), these bony structures started to become visible, which were surrounded externally by the periosteum (p). (10×, H&E).

in these data may be attributable to factors such as strain, health, age, diet, and management. The inner cellular layer of the perichondrium differentiated into osteoblasts by the 8th day in all experimental skeletal

tissue embryos, which is analogous to those published by Zorab and Salih (2021), who indicated that an intramembranous process immediately ossified the slender U-shaped clavicles on day 9. Some studies such

a, such Pourlis and Antonopoulos (2011), and Nakane and Tsudzuki (1999), stated were conducted seventh and eighth days, respectively. The first phalanx of the first digit remained cartilaginous during prechewing, a conclusion corroborated by Zorab and Salih (2021) in quail. Throughout the 10th day of incubation distinctly identified the condensation cells inside the deep avascular layer of the mesenchyme, noting a central core of rounded cells encircled by a layer of elongated cells. These results correspond with the work of Ahmed and Soliman (2013), who noted morphological alterations at this stage, characterized by enlargement and rounding of the cell body, whereas the cells inside the aggregate displayed traits of osteoprogenitor cells. Kürtül *et al.* (2009) previously showed that these cytological alterations lead to developed osteoblasts that release collagen and osteoid. The inner cellular layer of the perichondrium differentiated into osteoblasts by the 10th day in all embryos of Cb, Rp, Jq, and Cc, on 12th days, the mid-diaphysis area, where the chondrocytes had hypertrophied, the osteoblasts deposited osteoid tissue, forming a bone collar, and the progressive transformation of the perichondrium into the periosteum. This observation is consistent with the findings of Wu *et al.* (2022), who highlighted similar alterations in quail embryos over 10 days. The developed normal osteoblasts secrete a matrix that isolates rounder cells from one another in the middle region of the condensation. The matrix was osteoid, and the cells produced were osteoblasts. This suggests that throughout bone tissue creation, osteoblasts produce and deposit type I collagen, the principal protein component of the bone matrix (Shapiro, 2008). Additionally, Purlis *et al.* (1998) stated that the newly formed tissue undergoes vascularization, and the aggregated mesenchymal cells enlarge and become rounder, signifying that the cytological alterations lead to the differentiation of osteoblasts, which release collagen and osteoid matrix. On 14th day of incubation, osteoblasts were significantly augmented, and the deposition of the periosteal bone collar around the mid-diaphysis increased its thickness toward the center of the diaphysis. This finding is inconsistent with the observations of Purlis and Antonopoulos (2011) and corresponds with the study of Li *et al.* (2024), which demonstrated that osteoblasts not only generate osteoid matrix but also significantly contribute to its mineralization. This suggests that mature osteoblasts anchored inside the matrix differentiate into osteocytes. The ossification of the phalanx was observed on the 14th day, in contrast to Nakane and Tsudzuki *et al.* (1999) in Jq, who noted it on the 16th day. On the 16th day, mature osteoblasts were lodged in the matrix and differentiated into osteocytes, resulting in the formation of primary woven bone. Calcification of trabecular bone. The endochondral bone trabeculae continued to synthesize until they fused with the periosteal bone collar, encompassing the whole middiaphysis of the

humerus and establishing the principal ossification center (Wu *et al.*, 2022). Chondrocytes mineralize their surrounding matrix, providing a framework for the production of trabecular bone. They can also induce a bone collar, which is the precursor to cortical bone, in the neighboring perichondrium (Blumer, 2021). Shapiro (2008) reported that the collar gradually extended toward the proximal and distal epiphyses of long bones, ultimately encompassing the whole new bone. These findings suggest that ultimately, cartilage rods undergo erosion and alteration, resulting in the formation of the medullary cavity. Zorab and Salih (2021) reported that as the osteoid collar expands towards the ends of the long bone, the middiaphysis undergoes additional mineralization and converts into lamellar bone. Additionally, Li *et al.* (2024) reported that the long bones of the limbs undergo radial growth in the diaphysis. This expansion of growth occurs in the cortical bone via the formation of osteoblasts in the innermost coating of the periosteum (Al-Agele *et al.*, 2019). Furthermore, Shapiro (2008) revealed that a growing long bone comprises the epiphysis and metaphysis at both ends, with the diaphysis positioned in the center. The present investigation identified dense, randomly oriented regions of chondrocytes, particularly within hypertrophic and calcifying zones. This suggests that observable chondrocyte divisions indicate progressive thickening of the growth plate, resulting from the ongoing generation of residual chondrocytes and proliferation in adjacent zones, whereas the hypertrophic zone exhibits prominent, large chondrocytes within lacunae, interspersed by a dense matrix. The chondrocytes were clearly visible in the terminal zone next to the ossified regions. On day 18, the deceased chondrocytes were substituted by osteoids, which were secreted by osteoblasts and transported via substantial blood arteries inside the bone marrow, as stated by Prondvai *et al.* (2020). In the future, it's essential to undertake additional efforts to provide a comprehensive investigation of this issue, including multitissue examinations of nerves and/or muscles, as well as cross-species relative genes.

Conclusion

In conclusion, the present study provides histomorphometric data that reveal distinct patterns of embryonic skeletogenesis in precocial (Jq and Cc) and altricial (Rp and Cb) embryos. Morphometric examination of the ossified segments of the femur and humerus revealed that the length of the ossified region increased during the incubation period. The variations in ossification and chondrification were particularly evident in Jq. All bones in the FL and HL were ossified during incubation, except the patella. These findings may have practical implications, highlighting that HLs develop more rapidly than FLs in quail and other precocial embryos. Comparative embryological investigations across many species and features have

assembled considerable data on the timing of initial developmental events. To examine and comprehend the data gathered in this study, these statistics are crucial indicators and elements.

Acknowledgments

The authors extend their gratitude to the College of Veterinary Medicine, University of Diyala.

Conflict of interest

The authors confirm that they have no conflicts of interest.

Funding

This project was not supported by grants.

Authors' contribution

IMA: Writing original draft; RAA: supervision, conception, validation, writing, reviewing the manuscript.

Data availability

The data supporting this article's results are available in the manuscript and from PMN upon reasonable demand.

References

- Ahmed, Y.A. and Soliman, S.A. 2013. Long bone development in the Japanese quail (*Coturnix coturnix japonica*) embryos. Pak. J. Biol. Sci. 16(18), 911–919; doi:10.3923/pjbs.2013.911.919
- Al-Agele, R. 2020. The study of histological observations of ovine claw coronary region and the architecture morphology of arterial anastomosis of this area. Atatürk Univ. J. Vet. Sci. 15(1), 14–21; doi:10.17094/ataunivbd.634782
- Al-Agele, R.A. 2024. Comparative histomorphometrical study of the lamellae in odd-toed and even-toed ungulate animals. Iraqi J. Vet. Sci. 38(3), 701–706; doi:10.33899/ijvs.2024.148208.3565
- Al-Agele, R.A.A., Jabbar, A.I. and Al-Ubaidy, A.A.H. 2021. Study on morphohistological observations of the islets of langerhans in the pancreas of common wood pigeon *Columba palumbus*. Biochem. Cell. Arch. 21(1), 1165–1170.
- Al-Agele, R., Paul, E., Taylor, S., Watson, C., Sturrock, C., Drakopoulos, M., Atwood, R.C., Rutland, C.S., Menzies-Gow, N., Knowles, E. and Elliott, J. 2019. Physics of animal health: on the mechano-biology of hoof growth and form. J. R. Soc. Interface. 16(155), 1–12; doi:10.1098/rsif.2019.0214
- Augustine, S., Lika, K. and Kooijman, A.M. 2019. Altricial-precocial spectra in animal Kingdom. J. Sea Res. 143, 27–34; doi:10.1016/j.seares.2018.03.006
- Blumer, M.J. 2021. Bone tissue and histological and molecular events during development of the long bones. Ann. Anat. 235, 151704; doi:10.1016/j.aanat.2021.151704
- Chan, W.C., Tan, Z., To, M.K. and Chan, D. 2021. Regulation and role of transcription factors in osteogenesis. Int. J. Mol. Sci. 22(11), 5445; doi:10.3390/ijms22115445
- Dial, T.R. and Carrier, D.R. 2012. Precocial hindlimbs and altricial forelimbs: partitioning ontogenetic strategies in Mallard ducks (*Anas platyrhynchos*). J. Exp. Biol. 215, 3703–3710; doi:10.1242/jeb.057380
- Gao, J., Li, X., Zhang, Y. and Wang, H., 2018. Endochondral ossification in hindlimbs during Bufo gargarizans metamorphosis: a model of studying skeletal development in vertebrates. Dev. Dyn. 247(10), 1121–1134; doi:10.1002/dvdy.24669
- Gillian, D.M. 2000. Early ontogeny of locomotor behaviour: a comparison between altricial and precocial animals. Brain Res. Bull. 53(5), 719–726; doi:10.1016/S0361-9230(00)00404-4
- Ikedo, K. and Takeshita, S. 2016. The role of osteoclast differentiation and function in skeletal homeostasis. J. Biol. Chem. 159(1), 1–8; doi:10.1093/jb/mvv112
- Kadhim, T.J., Al-Agele, R.A.A. and Ibrahim, R.S., 2023. Histopathological study of the cecal tonsils post newcastle vaccine in broiler chickens. AIP Conf. Proc. 2475(1), 100008; doi:10.1063/5.0103023
- Kürtül, İ., Atalgin, Ş.H., Arslan, K. and Bozkurt, E.Ü. 2009. Ossification and growth of the bones of the wings and legs in prehatching period of the Hubbert strain broiler. Kafkas Univ. Vet. Fak. Derg. 15(6), 869–874; doi:10.9775/kvfd.2009.176
- Li, X., Zhang, Y. and Zhao, H. 2024. Endochondral ossification of hind limbs in embryonic development of Japanese Quail (*Coturnix japonica*). Avian Res. 15, 100152; doi:10.1016/j.avrs.2023.100152
- McGuire, R.S., Ourfalian, R., Ezell, K. and Lee, A.H. 2020. Development of limb bone laminarity in the homing pigeon (*Columba livia*). PeerJ 8, e9878; doi:10.7717/peerj.9878
- Nakamura, Y., Nakane, Y. and Tsudzuki, M. 2019. Skeletal development in blue-breasted quail embryos. Anim. Sci. J. 90(3), 353–365; doi:10.2741/4076
- Nakane, Y. and Tsudzuki, M. 1999. Development of the skeleton in Japanese quail embryos. DGD 41(5), 523–534; doi:10.1046/j.1440-169x.1999.00454.x
- Nasser, A.T., Al-Azzawi, A., Al-Agele, R. and Al-Ajeeli, K. 2024. Identification of extremely virulent infectious bursal disease virus via molecular and histological methods in broiler chickens. JWPR 14(1), 98–112; doi:10.36380/jwpr.2024.10
- Nie, C.H., Wan, S.M., Liu, Y.L., Liu, H., Wang, W.M. and Gao, Z.X. 2019. Development of teleost intermuscular bones undergoing intramembranous ossification based on histological-transcriptomic-proteomic data. Int. J. Mol. Sci. 20(19), 4698; doi:10.3390/ijms20194698
- Nishimura, R., Hata, K., Ono, K., Takashima, R., Yoshida, M. and Yoneda, T. 2012. Regulation of endochondral ossification by transcription factors. J. Oral Biosci. 54(4), 180–183; doi:10.2741/4076
- Pourlis, A.F. and Antonopoulos, J. 2011. The ossification of the pectoral girdle and fore limb skeleton of the

- quail (*Coturnix coturnix japonica*). Anat. Histolo Embryol. 40(3), 219–225; doi:10.1111/j.1439-0264.2011.01065.x
- Pourlis, A.F., Magras, I.N. and Petridis D. 1998. Ossification and growth rates of the limb long bones during the prehatching period in the quail (*Coturnix coturnix japonica*). Anat Histolo Embryol. 27(1), 61–73; doi:10.1111/j.1439-0264.1998.tb00157.x
- Prondvai, E., Witten, P.E., Abourachid, A., Huysseune, A. and Adriaens, D. 2020. Extensive chondroid bone in juvenile duck limbs hints at accelerated growth mechanism in avian skeletogenesis. J. Anat. 236(3), 463–473; doi:10.1111/joa.13109
- Prummel, K.D., Nieuwenhuize, S. and Mosimann, C. 2020. The lateral plate mesoderm. Development 147(12), dev175059; doi:10.1242/dev.175059
- Raggatt, L.J. and Partridge, N.C. 2010. Cellular and molecular mechanisms of bone remodeling. J. Biol. Chem. 285(33), 25103–25108.
- Salhotra, A., Shah, H.N., Levi, B. and Longaker, M.T. 2020. Mechanisms of bone development and repair. Nat. Rev. Mol. Cell. Biol. 21(11), 696–711; doi:10.1038/s41580-020-00279-w
- Sears, K., Maier, J.A., Sadier, A., Sorensen, D. and Urban, D.J. 2018. Timing the developmental origins of mammalian limb diversity. Genesis 56(1), e23079; doi:10.1002/dvg.23079
- Seki, R., Kamiyama, N., Tadokoro, A., Nomura, N., Tsuihiji, T., Manabe, M. and Tamura, K. 2012. Evolutionary and developmental aspects of avian-specific traits in limb skeletal pattern. Zoolog Sci. 29(10), 631–644; doi:10.2108/zsj.29.631
- Shapiro, F. 2008. Bone development and its relation to fracture repair. The role of mesenchymal osteoblasts and surface osteoblasts. Eur. Cell Mater. 15(53): e76; doi:10.22203/ecm.v015a05
- Watanabe, J. 2018. Clade-specific evolutionary diversification along ontogenetic major axes in avian limb skeleton. Evolution 72(12), 2632–2652; doi:10.1111/evo.13627
- Wei, X. and Zhang, Z. 2019. Ontogenetic changes of geometrical and mechanical characteristics of the avian femur: a comparison between precocial and altricial birds. J. Anat. 235, 903–911; doi:10.1111/joa.13062
- Wu, Q., Liu, H., Yang, Q., Wei, B., Wang, L., Tang, Q., Wang, J., Xi, Y., Han, C., Wang, J. and Li, L. 2022. Developmental transcriptome profiling of the tibial reveals the underlying molecular basis for why newly hatched quails can walk while newly hatched pigeons cannot. Front Cell Dev. Biol. 10, 745129; doi:10.3389/fcell.2022.745129
- Xu, X., Zhou, Z., Dudley, R., Mackem, S., Chuong, C.M., Erickson, G.M. and Varricchio, D.J. 2014. An integrative approach to understanding bird origins. Science 346(6215), 1253293; doi:10.1126/science.1253293
- Zorab, HK. and Salih, K.A. 2021. Development of the wing bones in quail's embryo; *Coturnix japonica*. Iraqi J. Vet. Sci. 35(1), 129–137; doi:10.33899/ijvs.2020.126438.1324.